Theor Chem Acc (2010) 127:493–506
DOI 10.1007/s00214-010-0738-2

REGULAR ARTICLE

Theoretical study on the role of cooperative solvent molecules in the neutral hydrolysis of ketene

Xiao-Peng Wu · Xi-Guang Wei · Xiao-Ming Sun · Yi Ren · Ning-Bew Wong · Wai-Kee Li

Received: 2 November 2009 / Accepted: 15 February 2010 / Published online: 4 March 2010

Abstract The results of a theoretical study of the reaction mechanism for the neutral hydration of ketene, $H_2C{=}C{=}O + (n + 1)\ H_2O \rightarrow CH_3COOH + nH_2O$ ($n = 0$–4), in solution are presented. All structures were optimized and characterized at the MP2(fc)/6-31 + G* level of theory, and then re-optimized by MP2(fc)/6-311 ++G**, and the effect of the bulk solvent is taken into account according to the conductor-like polarized continuum model (CPCM) using the gas MP2(fc)/6-311 ++G** geometries. Energies were refined for five-water hydration at higher level of theory, QCISD(T)(fc)/6-311 ++G**//MP2(fc)/6-311 ++G**. In the combined supermolecular/continuum model, one water molecule directly attacks the central C-atom, and the other four explicit water molecules are divided into two groups, one acting as catalyst(s) by participating in the proton transfer to reduce the tension of proton transfer ring, and the other being placed near the non-reactive oxygen or carbon atom in order to catalyze the hydration by engaging in hydrogen-bonding to the substrate (the so-called cooperative effect). Between the two possible nucleophilic addition reactions of water molecule, across the C=O bond or the C=C bond, the former one is preferred. Our calculations suggest that the favorable hydrolysis mechanism of ketene involves a sort of eight-membered ring transition structure formed by a three-water proton transfer loop, and a cooperative dimeric water near the non-reactive carbon-atom. The best-estimated in the present paper for the rate-determining barrier in solution, $\Delta G^{\neq}_{sol}$ (298 K), is about 58 kJ/mol, reasonably close to the available experimental result.

Keywords Ketene · Hydrolysis mechanism · Supermolecular/continuum model · Cooperative effect · Solvent effect

1 Introduction

Ketene, $H_2C{=}C{=}O$, is an interesting molecule in many respects. It is the simplest member of the ketene ($R_1R_2C{=}C{=}O$) family; it is also the simplest cumulene with oxygen being the heteroatom, and an isoelectronic species of allene ($H_2C{=}C{=}CH_2$) as well. Ketenes are important starting materials [1] and intermediates [2–5] in a variety of organic reaction, including rearrangement reactions [6], radical reactions [7], cycloaddition reactions [8–10], nucleophilic [11–13] and electrophilic [14, 15] additions, and acylation reactions [3, 5], etc. Ketene chemistry has been the subject of numerous investigations; the structures and properties of ketenes [16–19] are also of intense interest. Therefore, the study on the mechanism of ketenes reactions is also a desirable and timely project.

Electronic supplementary material The online version of this article (doi:10.1007/s00214-010-0738-2) contains supplementary material, which is available to authorized users.

X.-P. Wu · X.-G. Wei · X.-M. Sun · Y. Ren (✉)
College of Chemistry and Key State Laboratory of Biotherapy, Sichuan University, Chengdu 610064, People's Republic of China
e-mail: yiren57@hotmail.com

Y. Ren · N.-B. Wong (✉)
Department of Biology and Chemistry, City University of Hong Kong, Kowloon, Hong Kong
e-mail: bhnbwong@cityu.edu.hk

W.-K. Li
Department of Chemistry, The Chinese University of Hong Kong, Shatin, NT, Hong Kong

Scheme 1

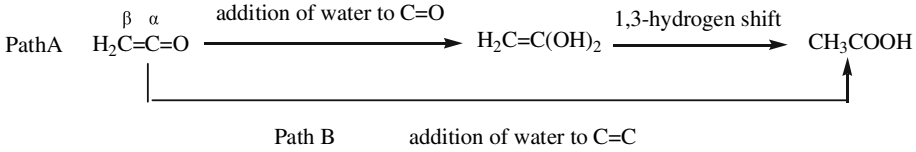

Hydration reactions of ketenes have been extensively studied experimentally [20–29] and computationally [30–33]. There are two possible reaction pathways (denoted as Path A and Path B, see Scheme 1) in the hydrolysis of ketene. The nucleophilic addition of the water molecule can first occur across the C=O bond, then the final product, acetic acid, is formed by intra-molecular hydrogen shift. In the alterative pathway, acetic acid is directly produced by the addition of water molecule across the C=C bond.

In an early experiment, Bothe and co-workers [20] reported the rate and mechanism of hydration of ketene in aqueous solution (pH = 4.4–9.85), and the measured activation enthalpy and entropy were 43.1 kJ/mol and −16 eu, respectively, leading to an activation Gibbs free energy of 63.0 kJ/mol. By ab initio methods using STO-3G and 4-31G basis sets, Nguyen et al. [31] made a molecular orbital study on the hydrolysis of ketene using a six-membered ring transition state (TS) model, in which one water molecule catalyzes the hydration by directly participating in the proton transfer. At the level of MP4(SDTQ)/6-31G*//RHF/6-31G*, Skancke [32] studied the addition of monomeric and dimeric water to ketene. Both of their calculations revealed that the preferred mode of addition of water dimer is across the C=O (rather than the C=C) bond of ketene. Nguyen et al. did not consider the second step of Path A (Scheme 1), but the results of Skancke showed that, in the addition of monomeric H_2O to ketene, the barrier of the second step of Path A is 191.2 kJ/mol in the gas-phase, higher than that of the first step of Path A (166.1 kJ/mol) and Path B (171.5 kJ/mol). In another paper by Nguyen et al. [33], new insights into the detailed mechanism of the hydration of ketene yielding acetic acid was obtained by ab initio calculations in the gas-phase at the level of QCISD(T)/6-31G**//MP2/6-31G** + ZPE(HF/6-31G**), and in solution by single-point calculations at MP2-PCM/6-31G** using the gas-phase MP2/6-31G** optimized geometries, respectively, and two- to four-water hydration pathways were investigated by the six-, eight- and ten-membered ring proton transfer TSs. Their results indicated that the hydration of ketene via an eight-membered ring TS structure is the most favorable reaction pathway. Also Path A (addition across the C=O bond) is preferred over Path B and the first step of Path A was also found to be rate-determining.

In recent studies on the hydration of cumulenes containing O, N and S as the hetero-atoms, such as O=C=O [34–38], O=C=S [39], S=C=S [40] and HN=C=NH [41–44], some new TS structures were proposed, yielding additional insights into the water-assisted hydrolysis mechanism. In the studies on the hydration of HN=C=NH, there are two different viewpoints for the position of the third water molecule in the three-water hydration model. Nguyen and coworkers thought that the third water molecule should be added to the proton transfer ring, and catalysis proceeds via an eight-membered ring TS structure [44]. Lewis et al. [41] proposed an alterative mechanism, i.e. the preferred three-water hydration involves a TS structure, in which only two water molecules participate in the six-membered proton transfer (PT) ring, and the third water molecule is near the non-reactive nitrogen atom, playing the cooperative role by engaging in hydrogen-bonding to the alcohol H-atom and to the imine-N of the forming isourea. Our theoretical studies on the neutral hydration of COS [39] and CS_2 [40] are consistent with the conclusion of Lewis et al. For example, the activation barrier for the rate-determining step of the two-water hydrolyses of CS_2 is 184.2 kJ/mol. When a water molecule is added near the non-reactive sulfur atom, the activation barrier decreases by about 30 kJ/mol, indicating that the cooperative catalytic third water molecule plays an important role in the hydrolysis reaction.

In view of that the cooperative effect was not discussed in the previous studies, in the present work, a detailed theoretical investigation on hydration of ketene in aqueous solution is carried out. In this study, five water molecules took part in the hydrolysis [Eq. (1)] and their roles are explicitly described. Bulk solvent effect is taken into account based on the conductor-like polarized continuum model (CPCM) [45] in order to estimate the salvation energies in aqueous solution ($\varepsilon = 78.4$), in which the whole molecular cavity is built up by the radii from the UFF force field [46]. In principle, the supermolecular geometries in bulk solvent should be different from those in the gas-phase, and we should do structural optimization in solvent. Unfortunately, we were not successful in getting converged results for some structures after numerous tries. Therefore, in the present paper, single-point calculations were carried out employing the optimized geometries in the gas-phase.

$$H_2C=C=O + (n+1)H_2O \rightarrow CH_3COOH + nH_2O \quad (n = 0\text{-}4) \qquad (1)$$

The main objectives of our study on the hydrolysis of ketene include the following: (a) to determine how many water molecules are actively involved; (b) to assess the cooperative effect of water molecules in this process; in

particular, to compare the performance of cooperative water molecules in different non-reactive regions; (c) to make a comparison between the hydration of ketene with that of carbon dioxide.

2 Computational details

All calculations were carried out using the Gaussian 03 set of programs [47]. The geometries of all pre-complexes (**M**), transition states (**TS**), intermediates (**In**) and products (**P**) were fully optimized initially at the MP2(fc)/6-31 + G* level, then they are re-optimized at MP2(fc)/6-311 ++G**. For the key structures in the most favorable pathway (five-water hydration), the high-level method of QCISD(T)/6-311 + G**//MP2/6-311 ++G** is used to refine the activation barriers. All optimized structures were characterized by vibrational frequency analysis at the MP2/6-31 + G* level. In the calculations of relative Gibbs free energies, a scaling factor 0.98 [48] was applied to the zero-point vibration energy corrections.

The catalytic effect of water molecules is interpreted by the changes of geometries and natural population analysis (NPA) [49] in the rate-determining step. The performance of hydrolysis of ketene in aqueous solution ($\varepsilon = 78.4$) was studied using the CPCM model employing the MP2/6-311 ++G** optimized geometries in the gas-phase. Throughout this paper, all bond lengths are in angstroms (Å) and bond angles are in degrees. All relative energies (in kJ/mol) refer to the Gibbs free energy changes, ΔG_{sol}, at 298 K with CPCM treatment.

3 Results and discussions

In the following discussions, species **M**, **TS**, **In** and **P** in Path A or Path B are assigned an italic prefix ***a-*** or ***b-***, respectively. These species are also given two subscripts, i and j ($i, j = 0$, 1, and 2), where "i" refers to the number of water molecules participating in the PT process, and "j" is the number of the cooperative water molecule(s).

The discussions consist of three parts. First, we present the influence of the number of explicit water molecules on the potential energy surface (PES) of the hydration of ketene in the presence of one to three water molecules participating in proton relay without explicit cooperative solvent molecule(s), i.e., $i = 0$–2 and $j = 0$. Then, we will add one or two water molecules, i.e., now j is 1 or 2, near the non-reactive carbon or oxygen atom in order to determine the cooperative effect of the solvent molecule on the energy barrier. Finally, we will compare the catalyzing effect of these two kinds of explicit water molecules.

3.1 Hydration of ketene without cooperative water molecule ($i = 0$–2; $j = 0$)

The hydration reactions, $H_2C{=}C{=}O + (n + 1)\ H_2O \rightarrow CH_3COOH + nH_2O$ ($n = i + j$, $i = 0$–2, $j = 0$), have been extensively examined [30–33]. In the present paper, to facilitate the comparison, we studied these pathways again at the MP2/6-311 ++G** level. Figures 1, 2, 3 illustrate the optimized structures of the stationary points and their main geometric features. The corresponding relative Gibbs free energies with CPCM treatment are also presented.

The hydration of ketene starts with the nucleophilic addition of a water molecule on the C_α atom, and a hydrogen atom of the water molecule transfers to the oxygen atom of ketene (Path A), or the addition takes place on the C_β atom of ketene (Path B). The final hydration product, acetic acid or hydrated acetic acid, is formed by 1,3-hydrogen shift (Path A) or in a direct fashion (Path B). Due to the similarity of the three cases studied in this section, here we only discuss the one-water hydrolysis of ketene (see Fig. 1).

There are two possible pre-coordination structures between one water molecule and ketene, ***a*-$\mathbf{M}_{0\text{-}0}$** and ***b*-$\mathbf{M}_{0\text{-}0}$**, corresponding to Path $A_{0\text{-}0}$ and $B_{0\text{-}0}$, respectively. For Path $A_{0\text{-}0}$, after the formation of pre-coordination complex ***a*-$\mathbf{M}_{0\text{-}0}$**, the nucleophilic addition of the water molecule across the $C_\alpha{=}O$ bond of ketene leads to ***a*-$\mathbf{TS}_{0\text{-}0}$** with a four-membered ring. The addition of H_2O to ketene is completed upon full proton transfer to ketenyl oxygen atom to form the intermediate, enediol (***a*-$\mathbf{In}_{0\text{-}0}$**). The final product of the one-water hydrolysis of ketene, acetic acid ($\mathbf{P}_{0\text{-}0}$), is formed via intramolecular 1,3-hydrogen shift TS, ***a*-$\mathbf{TS}'_{0\text{-}0}$**. For Path $B_{0\text{-}0}$, the nucleophilic addition of one water molecule across the $C_\alpha{=}C_\beta$ bond to form acetic acid via ***b*-$\mathbf{TS}_{0\text{-}0}$** with a four-membered ring.

It is noted that there is a significant geometric change for the $CH_2{=}C{=}O$ moiety accompanying the rehybridization at C_α ($sp \rightarrow sp^2$) and C_β ($sp^2 \rightarrow sp^3$) during the reaction, where the C_α–C_β bond is lengthened from 1.319 Å in ***a*-$\mathbf{M}_{0\text{-}0}$** via 1.335 Å in ***a*-$\mathbf{In}_{0\text{-}0}$** to 1.504 Å in $\mathbf{P}_{0\text{-}0}$ for path A; or from 1.320 Å in ***b*-$\mathbf{M}_{0\text{-}0}$** to 1.504 Å in $\mathbf{P}_{0\text{-}0}$ for path B. These trends are also seen in the two- and three-water hydration reactions of ketene.

Inspection of Figs. 1, 2, 3 shows that, for the pathways $A_{i\text{-}0}$ ($i = 0$–2), the activation Gibbs free energies of activation with the CPCM correction, $\Delta G^{\neq}_{sol}$, for the first step are 182.3 ($i = 0$), 100.3 ($i = 1$) and 72.1 ($i = 2$) kJ/mol. The tautomeric barriers of the second step are 177.3, 92.8 and 59.4 kJ/mol, respectively, which are lower than those of the first step by at least 4 kJ/mol. For pathways $B_{i\text{-}0}$ ($i = 0$–2), the reaction barriers are 195.4 ($i = 0$), 114.5 ($i = 1$), 82.1 ($i = 2$) kJ/mol. These results suggest that for

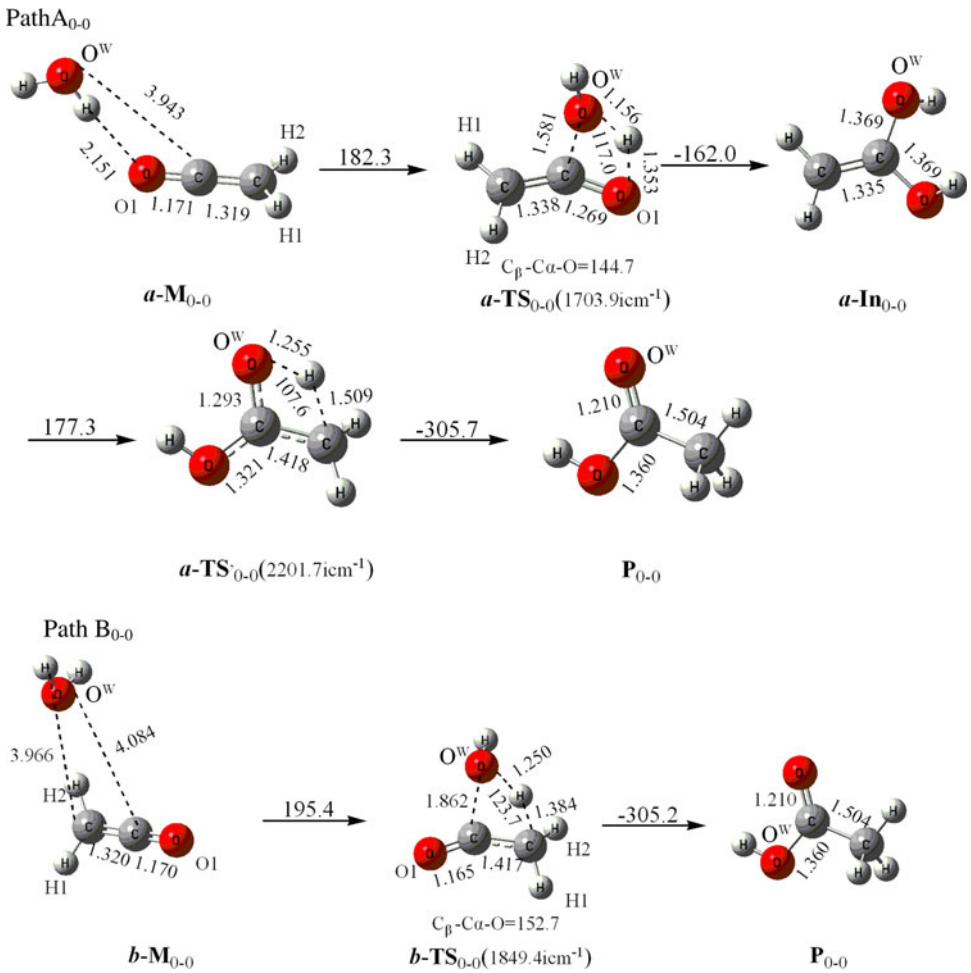

Fig. 1 MP2/6-311 ++G** structures of the stationary points and selected geometric parameters along the Paths $A_{0\text{-}0}$ and $B_{0\text{-}0}$ in the gas-phase. All bond lengths are in angstroms (Å) and bond angles are in degrees. The energy values (in kJ/mol) reported above the *arrows* are relative Gibbs free energies in solution, ΔG_{sol}, by single-point calculations at MP2-CPCM/6-311 ++G** using the gas-phase MP2/6-311 ++G** optimized geometries. The *numbers* in parentheses correspond to the sole imaginary frequency for each TS. Definitions are the same in the Figs. 2, 3, 5, 6, 7, 8, 11

one- to three-water hydrations of ketene: (1) the first step for C=O addition is rate-determining; (2) the barriers across the C=O bond are lower than those across the C=C bond by 13.1 ($i = 0$), 14.2 ($i = 1$) or 10.0 ($i = 2$) kJ/mol, indicating that Path A, i.e. addition across the C=O bond, is always kinetically favored; (3) with the incorporation of explicit water molecule(s), the rate-determining barriers decrease dramatically by 82.0 kJ/mol ($A_{0\text{-}0} \rightarrow A_{1\text{-}0}$) and 110.2 kJ/mol ($A_{0\text{-}0} \rightarrow A_{2\text{-}0}$) for the addition across the C=O bond or by 80.9 ($B_{0\text{-}0} \rightarrow B_{1\text{-}0}$) and 113.3 ($B_{0\text{-}0} \rightarrow B_{2\text{-}0}$) kJ/mol for the addition across the C=C bond. This can be attributed to the fact that the ring strain of TS is gradually reduced with the enlargement of PT ring and to the more comfortable hydrogen-bonding angles. An unrealistically high PT barrier in ***a*-TS**$_{0\text{-}0}$ or ***b*-TS**$_{0\text{-}0}$ may be attributed to the fact that a four-center TS is forbidden by orbital symmetry, and the need for more H_2O molecules to make the reaction concerted. Another factor may be the ring strain associated with the TS with a four-membered ring. Two-water hydration has one big advantage over the one-water hydration, but the two reacting centers are still not bridged in the TSs in the former reaction. Inclusion of the third water can make the PT process proceed more rapidly, implying ring strain in the rate-determining TS plays an important role in the hydration. Compared with two-water hydration, the rate-determining barrier for three-water hydration decreases by 28.2 kJ/mol for C=O addition or by 32.4 kJ/mol for C=C addition, giving an overall preference of 10.0 kJ/mol in favor of the former over latter. Our results are in good accord with the previous calculations [30, 31, 33].

In order to check if the obvious barrier differences exist between the single-point calculation and optimization in solution, we re-optimized two key mono-hydration structures in solution with the CPCM model, denoted as ***a*-M'**$_{0\text{-}0}$ and ***a*-TS'**$_{0\text{-}0}$ and shown in Fig. 4. It is found that optimization in solution only slightly modifies the activation barrier, and the barrier difference between single-point calculation and optimization in solution is less than 2 kJ/mol, suggesting that single-point calculation in solution using the gas-phase-optimized structure can give a reliable description for the hydration of ketene.

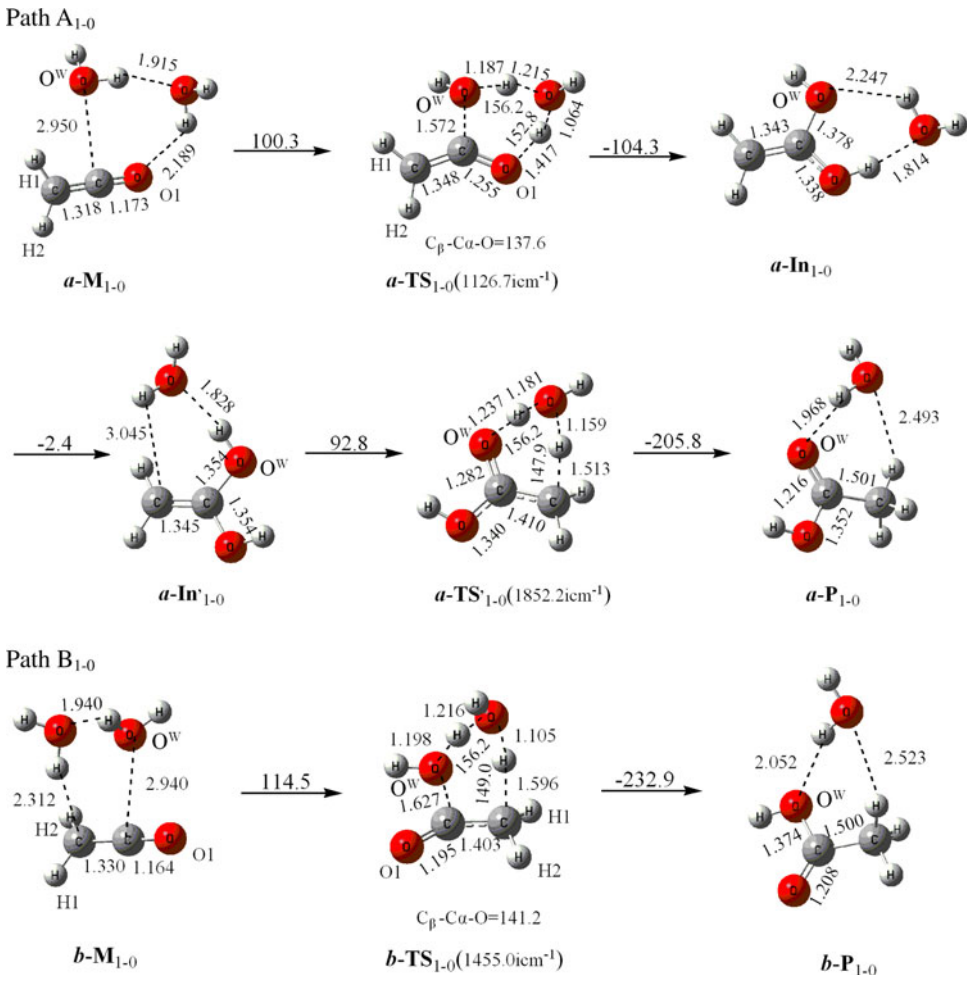

Fig. 2 MP2/6-311 ++G** optimized structures and relative Gibbs free energy values (in kJ/mol) of the stationary points along the two-water hydration pathways of ketene across the C=O bond (Path $A_{1\text{-}0}$) and the C=C bond (Path $B_{1\text{-}0}$) in solution without the explicit cooperative water molecule

3.2 Hydration of ketene in the presence of explicit cooperative water molecule(s) (j = 1-2)

In order to understand the cooperative effect in the hydration of ketene, one or two water molecules are placed near the non-reactive O-atom or C_β-atom, forming a six-membered ring or an eight-membered ring hydrogen bonding structure. First, we explore 2-, 3- and 4-water hydration with one cooperative water molecule. Subsequently, the cooperative effect induced by two water molecules in the four- and five-water hydration of ketene will be explored.

3.2.1 With one cooperative water molecule (i = 0–2, j = 1)

Building on the aforementioned discussions on the $A_{i,0}$, and $B_{i,0}$ (i = 0, 1 and 2), we now place one water molecule in the non-reactive region as a cooperative agent, and then study the hydration pathways $A_{i,1}$ and $B_{i,1}$ (i = 0, 1 and 2). All the optimized geometries and relative energies are presented in Fig. 5 ($i = 0, j = 1$), Fig. 6 ($i = 1, j = 1$) and Fig. 7 ($i = 2, j = 1$).

As shown in Fig. 5, for the two-water hydration in the presence of one cooperative water molecule, there are two pre-complexes, ***a*-M**$_{0\text{-}1}$ and ***b*-M**$_{0\text{-}1}$, corresponding to the addition across the C=O or C=C bond, respectively. For Path $A_{0\text{-}1}$, the first step remains the nucleophilic attack of the water molecule, through ***a*-TS**$_{0\text{-}1}$ with a four-membered ring to form ***a*-In**$_{0\text{-}1}$ with a PT $\Delta G^{\neq}_{sol}$ of 157.2 kJ/mol, lower than that of Path $A_{0\text{-}0}$ by 25.1 kJ/mol. In this process, the proton transfers from the oxygen atom of the water molecule to the ketenyl oxygen atom through a water chain. Then the reaction proceeds through the tautomeric TS structure, ***a*-TS'**$_{0\text{-}1}$, to reach the final monohydrated acetic acid, $CH_3COOH\cdots H_2O$ (***a*-P**$_{0\text{-}1}$), with a PT $\Delta G^{\neq}_{sol}$ of 92.8 kJ/mol, signifying that the first step is still rate-determining. Meanwhile, in Path $B_{0\text{-}1}$, monohydrated acetic acid (***b*-P**$_{0\text{-}1}$) is directly formed via a four-membered ring ***b*-TS**$_{0\text{-}1}$ with the $\Delta G^{\neq}_{sol}$ value of 182.6 kJ/mol, lower than that in Path $B_{0\text{-}0}$ by 12.8 kJ/mol. These results show that the activation barrier for the hydration of ketene can be

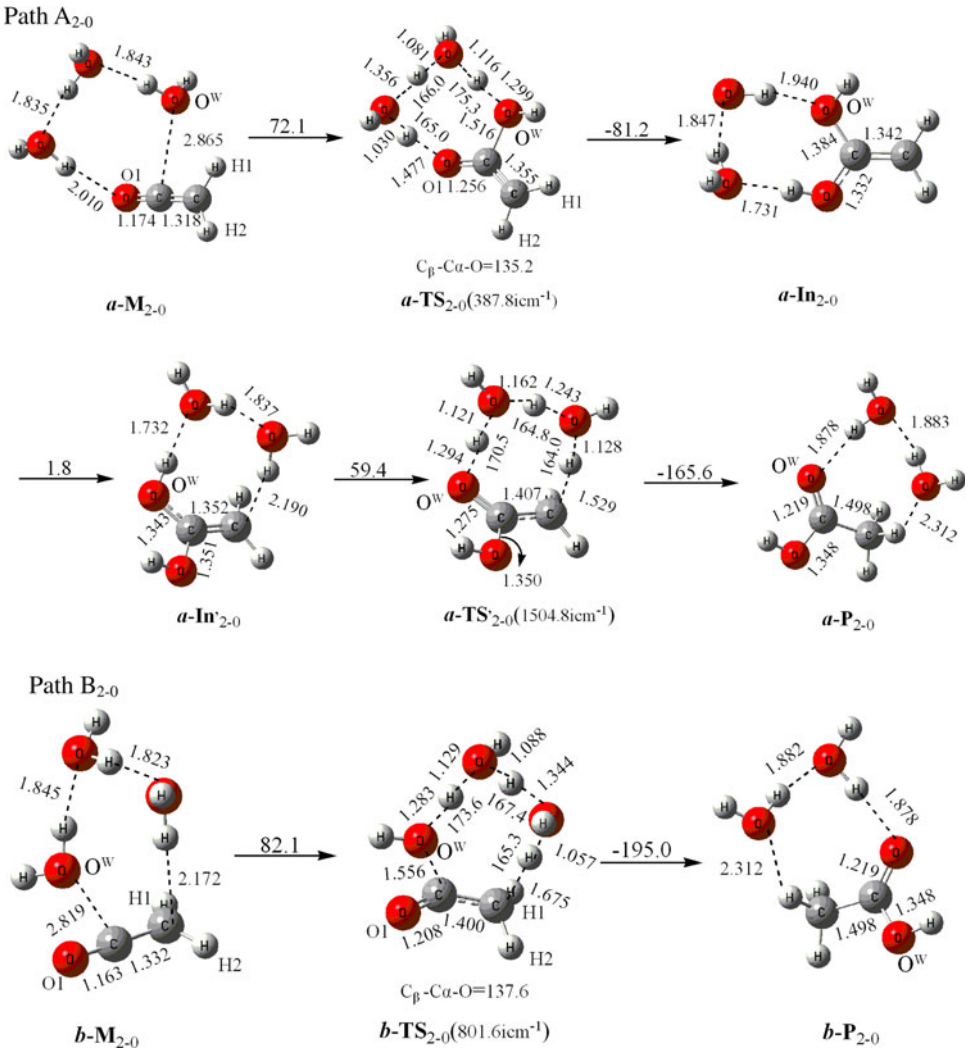

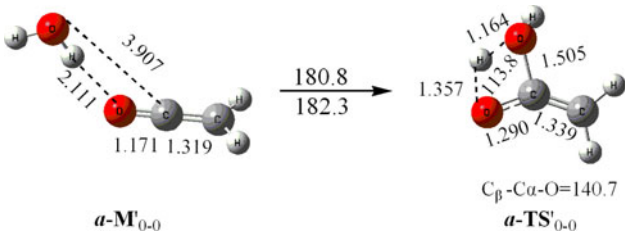

Fig. 3 MP2/6-311 ++G** optimized structures and relative Gibbs free energy values (in kJ/mol) of the stationary points along the three-water hydration pathways of ketene across the C=O bond (Path $A_{2\text{-}0}$) and the C=C bond (Path $B_{2\text{-}0}$) in solution without the explicit cooperative water molecule

Fig. 4 MP2-CPCM/6-311 ++G** optimized structures of the rate-determining step in the solvent for the first-step of one-water hydration of ketene across the C=O bond. The relative energy (in kJ/mol) reported above the arrows is the relative Gibbs free energy after the optimization in solvent and below the *arrows* is the corresponding ΔG_{sol} values employing the geometries in the gas-phase with CPCM correction

also reduced by forming a hydrogen-bonded six-membered ring with non-reactive C_β or O-atom. The changes of activation barriers can be explained by inspecting the TS structures. The distance of C_α–O^W (oxygen atom in the water molecule) in ***a*-TS**$_{0\text{-}1}$ is 1.518 Å, shorter than that in ***a*-TS**$_{0\text{-}0}$ by 0.063 Å, and the C_β–C_α–O angle in ***a*-TS**$_{0\text{-}1}$ is 141.5°, less than that in ***a*-TS**$_{0\text{-}0}$ by 3.2°. Similarly, the distance of C_α–O^W is shortened by 0.143 Å, and C_β–C_α–O angle is decreased by 5.3° from ***b*-TS**$_{0\text{-}0}$ to ***b*-TS**$_{0\text{-}1}$. All these geometric changes, induced by a hydrogen-bonded six-membered ring, can stabilize the rate-determining TS structures, ***a*-TS**$_{0\text{-}1}$ or ***b*-TS**$_{0\text{-}1}$, leading to lower reaction barriers.

In the three- and four-water hydration of ketene involving one cooperative water, the first step for the C=O bond addition is still rate-determining. For three-water process, the pre-complex $\mathbf{M}_{1\text{-}1}$ can lead to two possible TS structures, one across the C=O bond (***a*-TS**$_{1\text{-}1}$), and the other across the C=C bond (***b*-TS**$_{1\text{-}1}$), where the third water molecule is placed near the non-reactive carbon atom (Path $A_{1\text{-}1}$) or near the non-reactive oxygen atom (Path $B_{1\text{-}1}$). In the rate-determining step of across the C=O bond, the PT process takes place via a six-membered ring TS, characterized by a $\Delta G^{\neq}_{sol}$ value of 87.5 kJ/mol, lower than that found in Path $A_{1\text{-}0}$ by 12.8 kJ/mol. When the addition

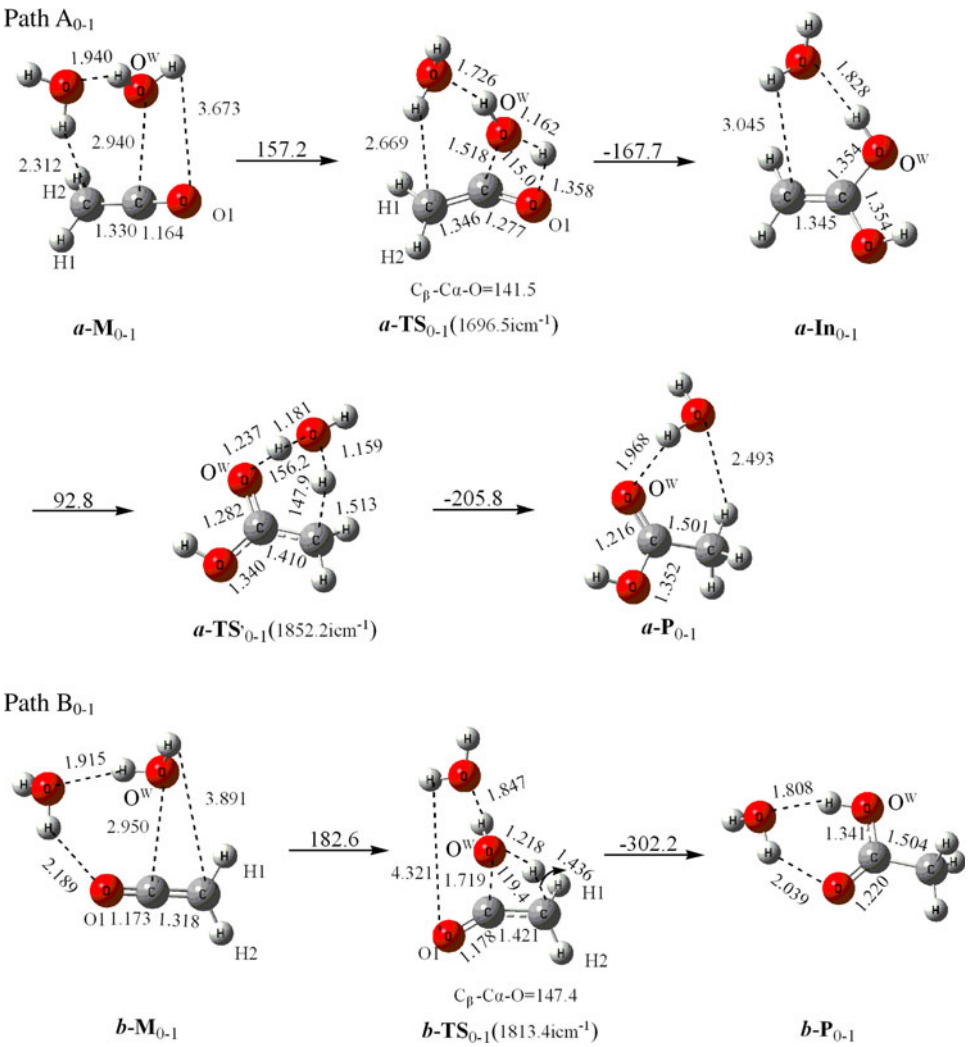

Fig. 5 MP2/6-311 ++G** optimized structures and relative Gibbs free energy values (in kJ/mol) of the stationary points along the two-water hydration pathways of ketene across the C=O bond (Path $A_{0\text{-}1}$) and the C=C bond (Path $B_{0\text{-}1}$) in solution with one explicit cooperative water molecule

occurs across the C=C bond, the third water molecule is involved in the hydrogen-bonded interactions with the non-reactive terminal oxygen, and the reaction barrier $\Delta G^{\neq}_{sol}$ of 103.8 kJ/mol is lower than that in Path $B_{1\text{-}0}$ by 10.7 kJ/mol, again indicating that the third water molecule plays an important role in the hydration as a cooperative agent instead of by assisting proton transfer. The variation of activation barrier could also be rationalized by the different rate-determining TS structures. Comparison between Paths $A_{1\text{-}0}$ and $A_{1\text{-}1}$ or between Paths $B_{1\text{-}0}$ and $B_{1\text{-}1}$ shows that the bond formation between C_α and O^W has progressed further with the placement of one water molecule near the non-reactive carbon or oxygen atom, and the C_α–O^W distance is reduced by 0.059 Å from ***a*-TS**$_{1\text{-}0}$ to ***a*-TS**$_{1\text{-}1}$, and 0.101 Å from ***b*-TS**$_{1\text{-}0}$ to ***b*-TS**$_{1\text{-}1}$, accompanying the decrease of the C_β–C_α–O angle from 137.6° in ***a*-TS**$_{1\text{-}0}$ to 134.1° in ***a*-TS**$_{1\text{-}1}$, or from 141.2° in ***b*-TS**$_{1\text{-}0}$ to 136.1° in ***b*-TS**$_{1\text{-}1}$.

Putting one explicit water molecule near the non-reactive carbon atom in ***a*-TS**$_{2\text{-}0}$ or near the non-reactive oxygen atom in ***b*-TS**$_{2\text{-}0}$ can lead to two eight-membered ring TSs for the four-water hydration reactions, ***a*-TS**$_{2\text{-}1}$ and ***b*-TS**$_{2\text{-}1}$. The aforementioned structural interpretation can be also applied to compare ***a*-TS**$_{2\text{-}1}$ with ***a*-TS**$_{2\text{-}0}$ or ***b*-TS**$_{2\text{-}1}$ with ***b*-TS**$_{2\text{-}0}$. The rate-determining barriers for Paths $A_{2\text{-}1}$ and $B_{2\text{-}1}$ are slightly reduced from ***a*-TS**$_{2\text{-}0}$ (72.1 kJ/mol) to ***a*-TS**$_{2\text{-}1}$ (69.0 kJ/mol), and from ***b*-TS**$_{2\text{-}0}$ (82.1 kJ/mol) to ***b*-TS**$_{2\text{-}1}$ (71.9 kJ/mol). Meanwhile, the distance of C_α–O^W is shortened from 1.516 Å in ***a*-TS**$_{2\text{-}0}$ to 1.478 Å in ***a*-TS**$_{2\text{-}1}$, and from 1.556 Å in ***b*-TS**$_{2\text{-}0}$ to 1.487 Å in ***b*-TS**$_{2\text{-}1}$, and angle C_β–C_α–O is reduced from 135.2° in ***a*-TS**$_{2\text{-}0}$ to 131.8° in ***a*-TS**$_{2\text{-}1}$, and from 137.6° in ***b*-TS**$_{2\text{-}0}$ to 133.2° in ***b*-TS**$_{2\text{-}1}$.

The results in Figs. 5, 6, 7 show that (1) one explicit water molecule can catalyze the hydration via a hydrogen-bonded TS formed by water and ketene instead of directly participating in proton transfer; (2) the first step of C=O bond addition is still rate-determining; (3) the addition across the C=O bond is favored over that across the C=C bond.

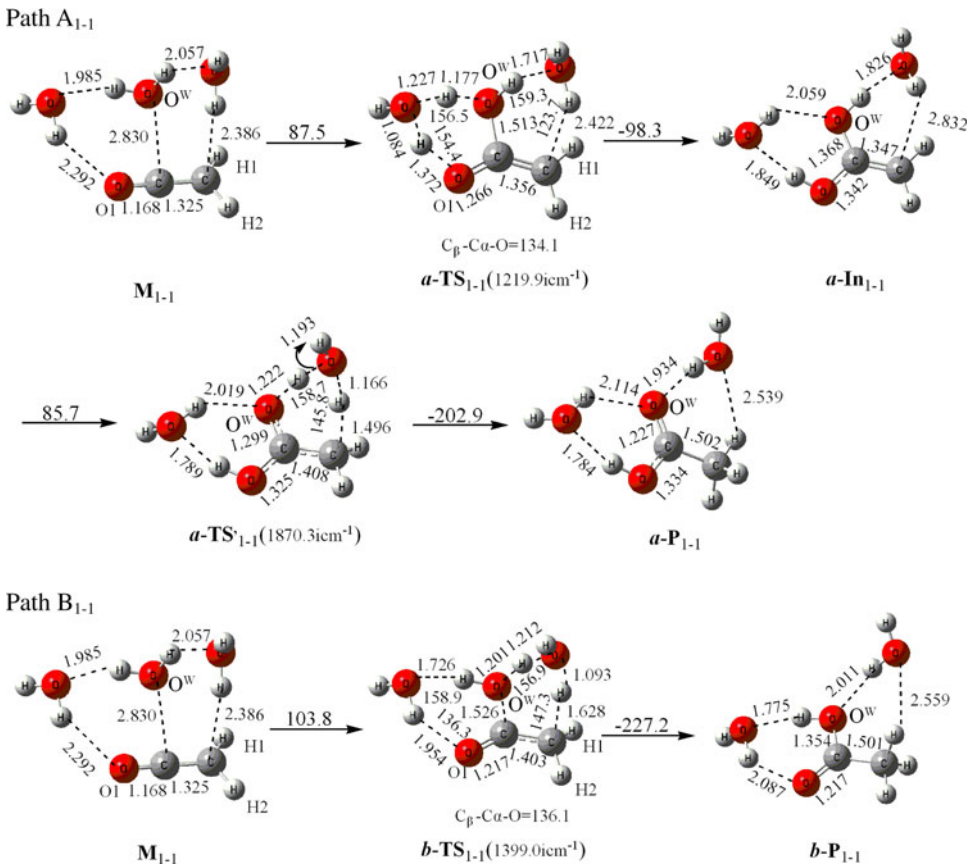

Fig. 6 MP2/6-311 ++G** optimized structures and relative Gibbs free energy values (in kJ/mol) of the stationary points along the three-water hydration pathways of ketene across the C=O bond (Path $A_{1\text{-}1}$) and the C=C bond (Path $B_{1\text{-}1}$) in solution with one explicit cooperative water molecule

3.2.2 *With two cooperative water molecules (i = 0–2, j = 2)*

The aforementioned results show that the energy activation barrier of the rate-determining step could also be reduced when one water molecule plays a cooperative role near the non-reactive region, instead of directly participating in the proton relay. The ensuing discussions will focus on what happens when two cooperative water molecules are involved in the hydration of ketene.

It is noteworthy from the aforementioned studies that four-membered ring TS structure is unfavorable due to unrealistically high PT barrier, and the first step of water addition is rate-determining. Hence, we only discuss the rate-determining step, i.e. the first step, for the four- and five-water hydration reactions involving a six- or eight-membered ring TS in the presence of two explicit water molecules.

In Path $A_{1\text{-}2}$ or $B_{1\text{-}2}$ (Fig. 8), the hydration of ketene starts with the pre-complex ***a*-M**$_{1\text{-}2}$ (same as ***b*-M**$_{2\text{-}1}$) or ***b*-M**$_{1\text{-}2}$ (same as ***a*-M**$_{2\text{-}1}$), and the reaction proceeds through a six-membered ring TS (***a*-TS**$_{1\text{-}2}$ or ***b*-TS**$_{1\text{-}2}$), in which a cooperative water dimer forms an eight-membered hydrogen-bonded structure with the substrate. The energy barriers are 76.6 (***a*-TS**$_{1\text{-}2}$, C=O addition) and 93.3 kJ/mol (***b*-TS**$_{1\text{-}2}$, C=C addition), lower than ***a*-TS**$_{1\text{-}1}$ and ***b*-TS**$_{1\text{-}1}$ by 10.9 and 10.5 kJ/mol, respectively, indicating that the cooperative effect induced by an eight-membered ring hydrogen-bonded structure is more pronounced than by a six-membered ring one. These results may be attributed by two structural features in ***a*-TS**$_{1\text{-}2}$ and ***b*-TS**$_{1\text{-}2}$, one is the angle of hydrogen bonds, and the other is the distance of C_α–O^W. In the non-reactive region of ***a*-TS**$_{1\text{-}2}$ or ***b*-TS**$_{1\text{-}2}$, there are three hydrogen bonds, where the angles are 158.4°, 159.4° and 171.9° for the C=O addition, and 160.4°, 160.5° and 176.1° for the C=C addition, more toward linearity than those found in ***a*-TS**$_{1\text{-}1}$ (123.7°, 159.3°) or ***b*-TS**$_{1\text{-}1}$ (136.3°, 158.9°). Moreover, the C_α–O^W distance is remarkably reduced from 1.513 Å in ***a*-TS**$_{1\text{-}1}$ to 1.483 Å in ***a*-TS**$_{1\text{-}2}$ or from 1.526 Å in ***b*-TS**$_{1\text{-}1}$ to 1.493 Å in ***b*-TS**$_{1\text{-}2}$. All of these geometrical changes will stabilize ***a*-TS**$_{1\text{-}2}$ and ***b*-TS**$_{1\text{-}2}$.

Compared with the one- up to four-water hydration, the most favorable reaction pathway seems to involve an eight-membered ring TS ***a*-TS**$_{2\text{-}2}$ (Path $A_{2\text{-}2}$) or ***b*-TS**$_{2\text{-}2}$ (Path $B_{2\text{-}2}$) in the five-water hydration of ketene (Fig. 9), where nearly perfectly oriented hydrogen bonds (with angles ranging from 163.8° to 176.4°) exist in the proton relay region. Meanwhile, another hydrogen-bonded eight-membered ring in the non-reactive region will induce the two

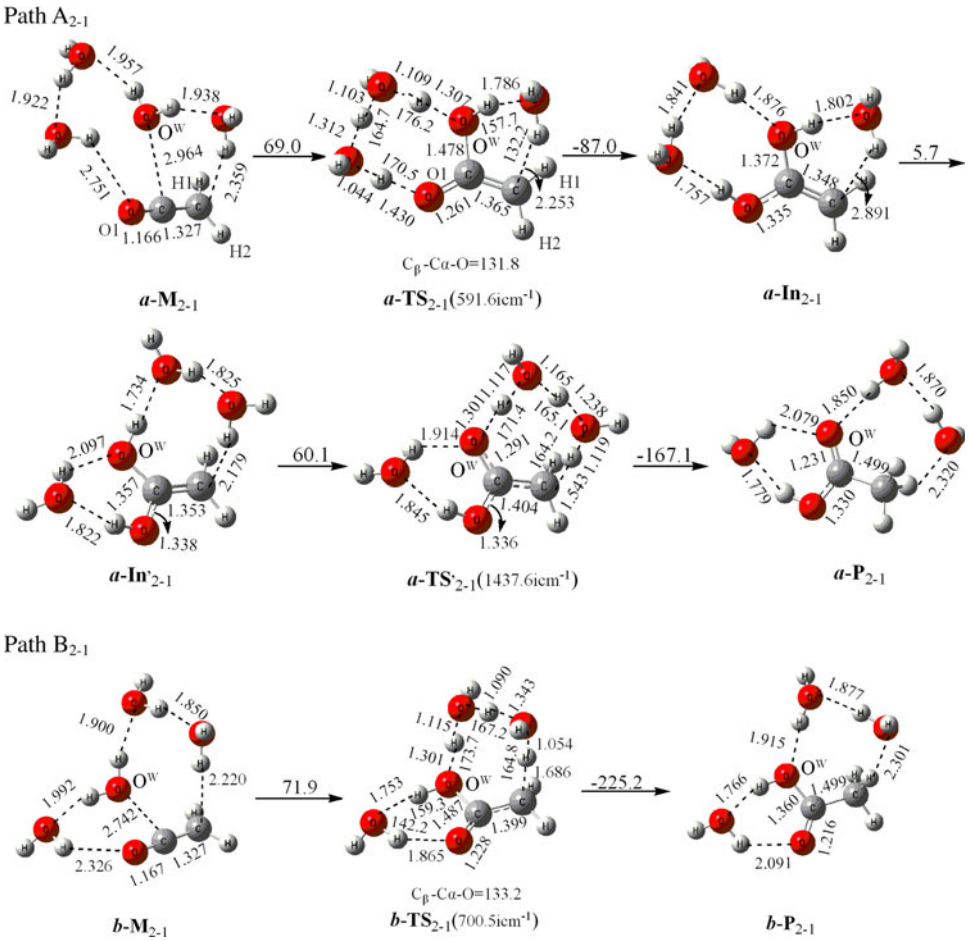

Fig. 7 MP2/6-311 ++G** optimized structures and relative Gibbs free energy values (in kJ/mol) of the stationary points along the four-water hydration pathways of ketene across the C=O bond (Path $A_{2\text{-}1}$) and the C=C bond (Path $B_{2\text{-}1}$) in solution with one explicit cooperative water molecule

TSs to be tighter than others in the present study, as shown from the shorter distance of C_α–O^W (1.453 Å in ***a*-TS**$_{2\text{-}2}$ and 1.461 Å in ***b*-TS**$_{2\text{-}2}$). Rehybridization at C_α has also progressed further than other TSs, accompanying the smaller C_β–C_α–O angle of 130.4° for ***a*-TS**$_{2\text{-}2}$ or 131.9° for ***b*-TS**$_{2\text{-}2}$. The rate-determining barrier is 49.9 kJ/mol for Path $A_{2\text{-}2}$ or 58.0 kJ/mol for $B_{2\text{-}2}$, lower than all others in the present study. As in earlier discussions, we again have the confirmation that addition across the C=O bond is favored.

The energy barriers in solution for the rate-determining step in the hydrolysis of ketene with one to five water molecules are summarized in Table 1, and Fig. 10 shows the trend of the rate-determining activation Gibbs free energies of activation with CPCM correction along the increase of the explicit water molecule(s) in the hydration of ketene.

Inspection of Table 1 shows that the five-water hydrolysis pathway involving a dual eight-membered ring TS structure is most the favorable among the reactions studied in this work, and the refined activation barrier, 57.5 kJ/mol, at the level of QCISD(T)/6-311 + G**// MP2/6-311 ++G** with the MP2-CPCM/6-311 ++G** correction, is reasonably close to the experimental result of 63.0 kJ/mol [20].

3.3 Further comparison of geometries and activation barriers among the hydration pathways of ketene

In the hydrolysis of ketene, the rate-determining activation barriers in solution, $\Delta G^{\neq}_{sol}$, at the level of MP2-CPCM/6-311 ++G**//MP2/6-311 ++G** generally decrease with the increment of the number of water molecules. Comparison of one- to five-water hydrations indicates that the barrier depends on the number of water molecules directly participating in the proton transfer and the number of the cooperative water molecules in the non-reactive region. Taking the six-membered ring TSs across the C=O bond as an example, $\Delta G^{\neq}_{sol}$ decreases with the increase of non-reactive waters in the following order: 100.3 (***a*-TS**$_{1\text{-}0}$, $i = 0$) > 87.5(***a*-TS**$_{1\text{-}1}$, $i = 1$) > 76.6 kJ/mol (***a*-TS**$_{1\text{-}2}$, $i = 2$), suggesting that two water molecules near the non-reactive region give rise to more effective cooperative effect than one water molecule. If we fix two water molecules in the non-reactive region,

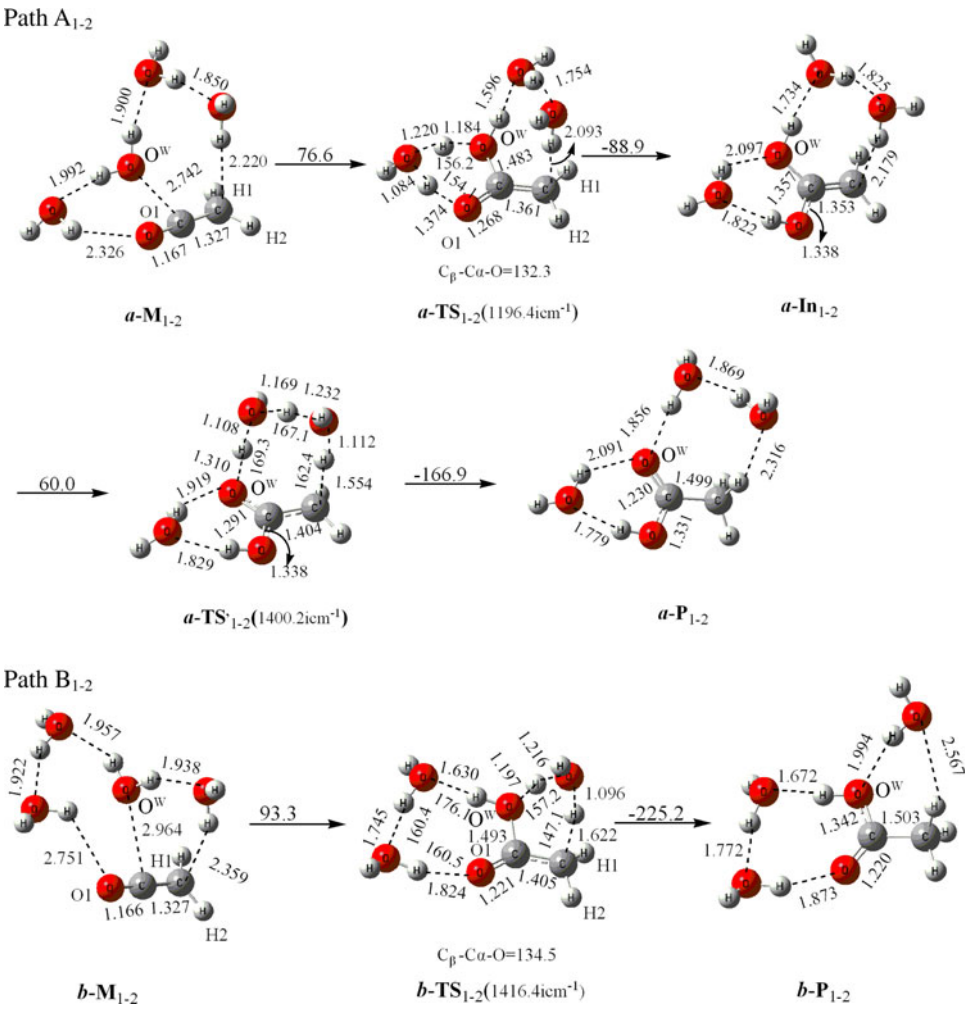

Fig. 8 MP2/6-311 ++G** optimized structures and relative Gibbs free energy values (in kJ/mol) of the stationary points along the four-water hydration pathways of ketene across the C=O bond (Path $A_{1\text{-}2}$) and the C=C bond (Path $B_{1\text{-}2}$) in solution with two explicit cooperative water molecule

i.e., $j = 2$, and only discuss the TSs across the C=O bond, it is found that the barriers decease from 76.6 (six-membered ring ***a*-TS**$_{1\text{-}2}$) to 49.9 kJ/mol (eight-membered ring ***a*-TS**$_{2\text{-}2}$), showing that the hydrolysis of ketene via a sort of eight-membered ring TS is the most favorable due to the better catalytic effect of the three-water chain. These interesting results can be rationalized by the geometrical features of the TSs by comparing the hydrogen bonds and the C_α–O^W distances in the rate-determining TS structures. Although it is difficult to detect the geometry of a hydrogen bond, a statistical analysis of X-ray crystallographic data has shown that most effective hydrogen bonds in crystals deviate from linearity by 10–15°. The angles of hydrogen bond in the proton relay region of ***a*-TS**$_{2\text{-}2}$ range from 165° to 176°, more reasonable than those in the ***a*-TS**$_{1\text{-}2}$ (154°–156°). Due to the less repulsion among three heavy atoms with higher electronegativity in ***a*-TS**$_{2\text{-}2}$ and less stabilization of ***a*-TS**$_{1\text{-}2}$, there is a lower barrier in the five-water hydrolysis process of ketene than that in the four-water hydrolysis by 28.7 kJ/mol for the addition taking place across the C=O bond.

All of our calculations indicate that the rate-determining barrier for the C=O addition is always lower than the corresponding one for the C=C addition. In other words, nucleophilic addition across the C=O bond in the hydration of ketene is more favorable than across the C=C bond. These results can be interpreted by electrostatic potential (ESP) analysis of parent ketene, where the ESP value in the region around the oxygen atom is more negative, implying the oxygen atom bearing lone pair of electrons is electron-rich and the electrophilic attack will occur more easily by proton at oxygen. Meanwhile, the terminal oxygen atom is also less steric hindered, which will favor the proton to transfer from water molecule to oxygen atom.

The variation of activation barriers can be also explained by electrical relaxation associated with the formation of rate-determining TS. Here, we only discuss the addition across C=O bond. With the attacking of water molecule toward the central carbon atom of ketene (C_α), the electrons will transfer from the water molecule cluster to the H_2CCO moiety for the process ***a*-M**$_{i\text{-}j}$ → ***a*-TS** $_{i\text{-}j}$. The lower activation barrier will be induced by the more

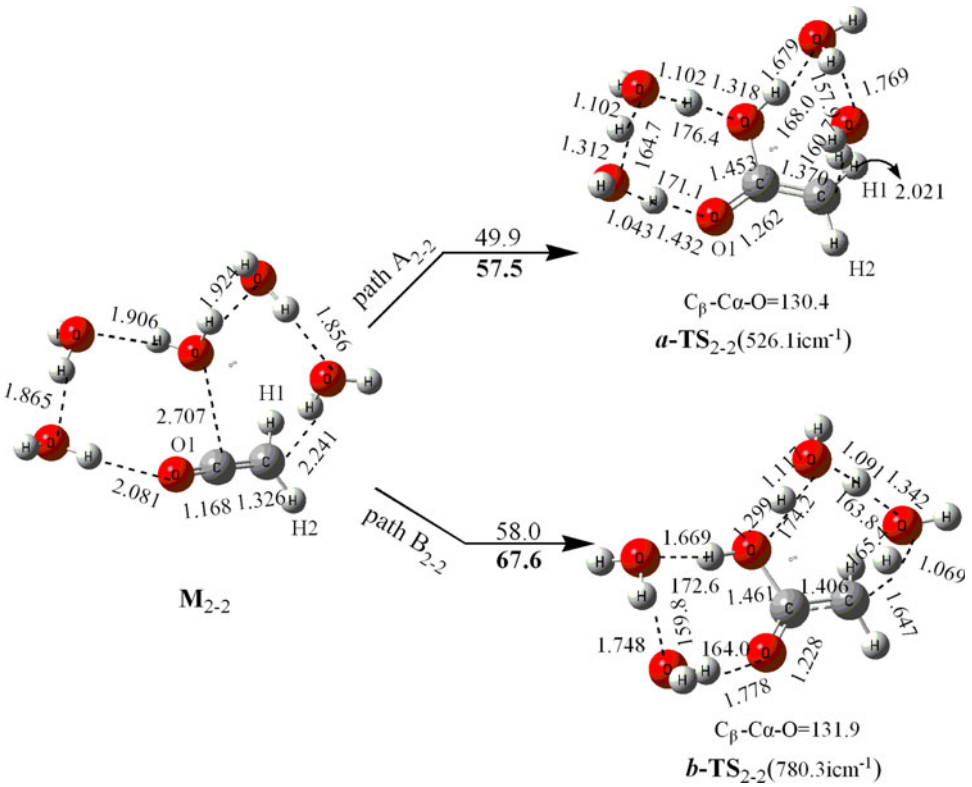

Fig. 9 MP2/6-311 ++G** optimized structures and rate-determining activation Gibbs free energies (in kJ/mol) of the stationary points for the five-water hydration of ketene across the C=O bond (Path $A_{2\text{-}2}$) and the C=C bond (Path $B_{2\text{-}2}$) in solution with two explicit cooperative water molecule. The energy values (in kJ/mol) reported below the *arrows* are the relative Gibbs free energies, ΔG_{sol}, at the level of QCISD(T)/6-311 ++G**//MP2/6-311 ++G** with the MP2-CPCM correction, whereas above the *arrows* are the ΔG_{sol} values at MP2-CPCM/6-311 ++G**//MP2/6-311 ++G**

Table 1 Energy activation barriers $\Delta G_{sol}^{\neq}$ (kJ/mol) for the first step in the hydration of ketene in aqueous solvent

	Pathway	C=O addition	Pathway	C=C addition
$H_2C{=}C{=}O + H_2O$	A_{00}	182.3[a]	B_{00}	195.4[a]
$H_2C{=}C{=}O + 2H_2O$	A_{01}	157.2[a]	B_{01}	182.6[a]
	A_{10}	100.3[b]	B_{10}	114.5[b]
$H_2C{=}C{=}O + 3H_2O$	A_{11}	87.5[b]	B_{11}	103.8[b]
	A_{20}	72.1[c]	B_{20}	82.1[c]
$H_2C{=}C{=}O + 4H_2O$	A_{12}	76.6[b]	B_{12}	93.3[b]
	A_{21}	69.0[c]	B_{21}	71.9[c]
$H_2C{=}C{=}O + 5H_2O$	A_{22}	49.9[c]	B_{22}	58.0[c]
		57.5[d]		67.6[d]

[a] Four-membered ring rate-determining TS

[b] Six-membered ring rate-determining TS

[c] Eight-membered ring rate-determining TS

[d] Refined barriers at the level of QCISD(T)/6-311 ++G**//MP2/6-311 ++G**

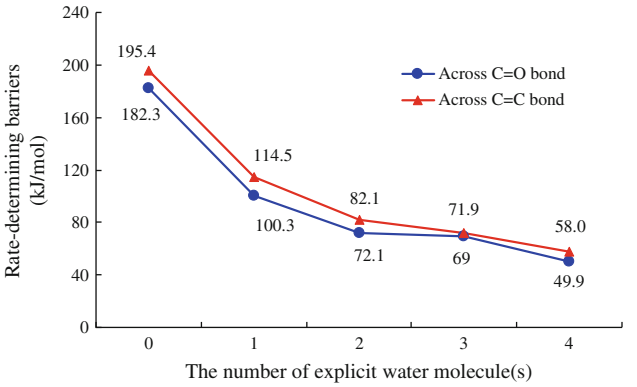

Fig. 10 The trend of the rate-determining activation Gibbs free energies at the level of MP2/6-311 ++G** with MP2-CPCM/6-311 ++G** correction as a function of the explicit water molecule(s) in the hydration of ketene through four-, six-, eight-membered ring proton relay, in the presence of 0–2 cooperative water molecules. Only the results of the favorable pathways in the two-water ($A_{1,0}$ and $B_{1,0}$), three-water ($A_{2,0}$ and $B_{2,0}$) and four-water ($A_{2,1}$ and $B_{2,1}$) hydration reactions are reported. Orange line is for the addition across the C=O bond, and blue line is for the C=C bond addition

negative Δq values, defined as $q(H_2CCO$ in TS)–$q(H_2CCO$ in pre-complex), with the increase in the number of explicit water molecule(s). This prediction was supported by the NPA charge changes presented in Table 2, where the Δq values gradually become more negative from one-water to five-water hydration, accompanying the decrease of C_α–O^W bond and the lowering of rate-determining Gibbs free energies of activation.

A closer inspection of activation barriers in Figs. 1, 2, 3, 4, 5, 6, 7, 8 and 9 reveals that the hydration of ketene can be catalyzed by two functions, one by reducing the strain of proton transfer ring, the other through the hydrogen-bonding formed by water molecules and terminal atom. It will be interesting to compare the relative merits of these two effects: the question is which one is more important, or

Table 2 Selected NPA charge changes of the H_2CCO moiety from pre-complexes to the rate-determining TSs, $\Delta q(H_2CCO)$, the corresponding MP2-CPCM/6-311 ++G(d, p)//MP2/6-311 ++G(d, p) activation Gibbs free energies (kJ/mol) in solution, $\Delta G^{\neq}_{sol}$, and the O^W–C_α distance(Å), $r(O^W–C_\alpha)$, in the rate-determining TSs

Pathway A_{i-j}	A-M_{i-j} → a-TS $_{i-j}$	$\Delta q(H_2CCO)$	$\Delta G^{\neq}_{sol}$	$R(O^W–C_\alpha)$
$I = 0, j = 0$	***a*-M**$_{0-0}$ → ***a*-TS**$_{0-0}$	–0.268	182.3	1.581
$i = 1, j = 0$	***a*-M**$_{1-0}$ → ***a*-TS**$_{1-0}$	–0.326	100.3	1.571
$i = 2, j = 0$	***a*-M**$_{2-0}$ → ***a*-TS**$_{2-0}$	–0.408	72.1	1.516
$i = 2, j = 1$	***a*-M**$_{2-1}$ → ***a*-TS**$_{2-1}$	–0.431	69.0	1.478
$i = 2, j = 2$	**M**$_{2-2}$ → ***a*-TS**$_{2-2}$	–0.437	49.9	1.453

are they comparable? For the three-water hydration of ketene, there are two possible reaction pathways. The third water molecule could be added to the proton transfer ring to form a TS with an eight-membered ring, ***a*-TS**$_{2-0}$ or ***b*-TS**$_{2-0}$. Alternatively, the water-assisted hydrolysis of ketene involves a TS with a six-membered proton transfer ring, and the third water molecule is located near the non-reactive region to engage in hydrogen-bonding to the alcohol H-atom and to the terminal carbon, C_β, in ketene (***a*-TS**$_{1-1}$), or the terminal oxygen in ketene (***b*-TS**$_{1-1}$). It is found that the rate-determining barrier for A_{2-0} or B_{2-0} is significantly lower than that for A_{1-1} or B_{1-1} by 15.4 kJ/mol (Path A) or 21.7 kJ/mol (Path B) kJ/mol, showing that cooperative effect induced by the water molecule in the non-reactive region is considerably weaker than that from the directly catalyzing through water chain, even though neither roles can be neglected. Such phenomenon may be attributed to the larger dipole moment of ***a*-TS**$_{2-0}$ (5.12 D) or ***b*-TS**$_{2-0}$ (5.02 D) than that of ***a*-TS**$_{1-1}$ (3.34 D) or ***b*-TS**$_{1-1}$ (2.61 D). Hence the polar medium would stabilize those TS structures with higher dipole moment, thus lowering the activation barrier and speeding up the hydration process of ketene in aqueous solution. This situation is also observed in the comparison between A_{2-1} and A_{1-2} or B_{2-1} and B_{1-2}. The present results are different from those in the three-water hydrolysis of CO_2 [38], COS [39], CS_2 [40] and NH=C=NH [41, 42], where the TS structures with lower barrier involve a six-membered proton ring formed by a water dimer, and the third water molecule is near the non-reactive nitrogen atom playing the cooperative role.

3.4 Comparison between the hydration of ketene with that of carbon dioxide

Ketene can be viewed as an analog of carbon dioxide, in which one of oxygen atoms is substituted by a CH_2 group. Thus, it is of interest to compare the performance of cooperative solvent in the hydration reactions of these two compounds. Many studies on the neutral hydration of CO_2 have been reported [34–38], where the third explicit water molecule prefers to be located in the non-reactive region, involving a rate-determining six-membered ring instead of an eight-membered ring TS structure, similar to pathway A_{1-1} or B_{1-1} in the present study. In order to stress the importance of cooperative effect of solvent for the hydration of CO_2, here we have calculated the three- and five-water hydrations of carbon dioxide using MP2/6-311 ++G** method with MP2-CPCM correction, where the pre-complexes and TSs are denoted as CO_2-**M**$_{2-0}$ or CO_2-**M**$_{2-2}$ and CO_2-**TS**$_{2-0}$ or CO_2-**TS**$_{2-2}$, respectively, and made a comparison with the corresponding hydration pathways of ketene at the same level. The optimized structures of CO_2-**M**$_{2-0}$, CO_2-**M**$_{2-2}$ CO_2-**TS**$_{2-0}$, and CO_2-**TS**$_{2-2}$**,** as well as the $\Delta G^{\neq}_{sol}$ values are presented in Fig. 11, which show that the Gibbs free energy of activation in aqueous solution is 88.8 kJ/mol for the five-water hydration of carbon dioxide, lower than that in the three-water hydration of carbon dioxide by about 20 kJ/mol. Meanwhile, the C_α–O^W distance (1.456 Å) in CO_2-**TS**$_{2-2}$ is shorter than that that in CO_2-**TS**$_{2-0}$ (1.547 Å), and a more negative value of Δq (−0.457), q(CO_2 in CO_2-**TS**$_{2-2}$)–q(CO_2 in CO_2-**M**$_{2-2}$), is observed, whereas the difference of q(CO_2 in CO_2-**TS**$_{2-0}$) with q(CO_2 in CO_2-**M**$_{2-0}$) is -0.378. These results reveal that the five-water hydrolysis is more favorable than the three-water hydration of carbon dioxide when there exists a rate-determining TS structure involving an eight-membered proton transfer ring, and other two water molecules located in the non-reactive region playing the cooperative role. It is worth noting that the $\Delta G^{\neq}_{sol}$ values for the hydration of ketene are always much lower than those of carbon dioxide, showing the hydration of ketene is more facile. This phenomenon can be attributed their different O-protonation energies. Our calculations show that the O-protonation of CH_2=C=O is more exothermic than that of O=C=O by 68.2 kJ/mol, implying that the oxygen atom in CH_2=C=O is a better proton acceptor. Thus, the proton transfer from water to the oxygen atom in ketene is more favorable than that in carbon dioxide, leading to a lower the rate-determining barrier.

4 Concluding remarks

In this work, a comprehensive mechanistic investigation of the hydrolysis of ketene has been carried out using ab initio methods. The studied reaction systems include up to four explicit water molecules, and the effect of water bulk solvent is taken into account using the CPCM model. In all the studied pathways, the nucleophilic addition across the C=O bond is always favored, and the first step, involving proton transfer from the attacking water to oxygen of ketene, is rate determining. The hydration of CH_2=C=O can be significantly catalyzed by proton relay, but the

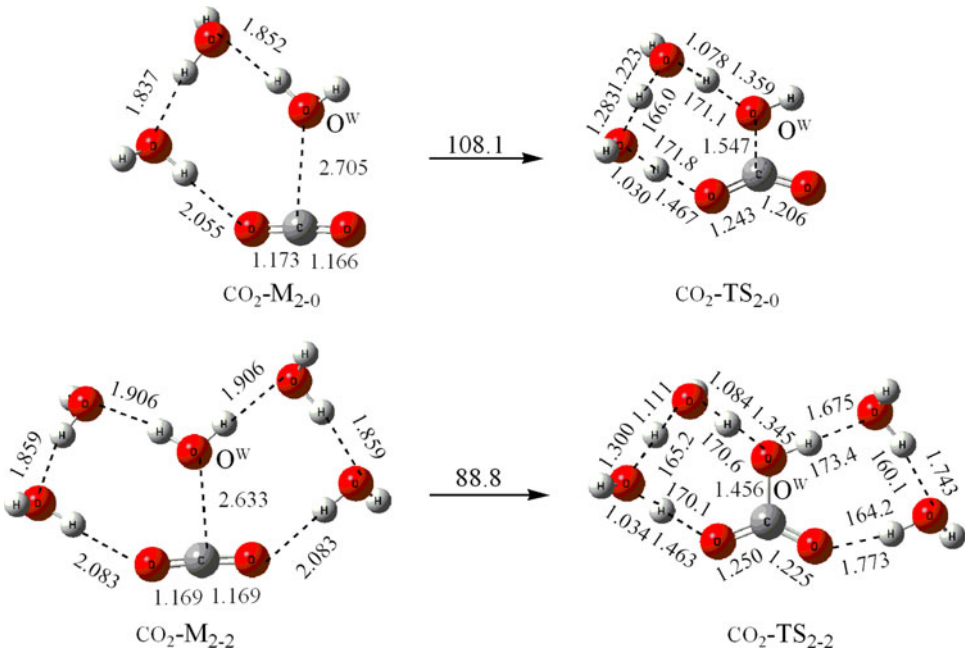

Fig. 11 MP2/6-311 ++G** optimized structures of the stationary points for the first step of three- and five-water hydrations of carbon dioxide. The energy values (in kJ/mol) above the *arrows* are the Gibbs activation free energy with CPCM correction

cooperative role induced by the solvent molecule(s) in the non-reactive region cannot be ignored, even though the latter is less important. The catalytic effect of the water molecule(s) can be explained by the structural and electrical features of rate-determining TSs. It is worth noting that our proposed models for the three-water hydration of ketene are different from those found in the hydration of CO_2 [38] and HN=C=NH [42] by Lewis et al.; they previously suggested that the third water molecule would participate in hydrogen bonding in a TS having two fused six-membered rings (see ***a*-TS**$_{1\text{-}1}$ of Path $A_{1\text{-}1}$ in Fig. 6). On the other hand, our results indicate that the third water molecule is likely to take part in the proton transfer through an eight-membered ring TS with a larger dipole moment (see ***a*-TS**$_{2\text{-}0}$ of Path $A_{2\text{-}0}$ in Fig. 3). The most favorable hydration pathway may involve a dual eight-membered ring TS in the five-water model, where proton prefers transferring to ketenyl oxygen atom by a three-water chain, and another dimeric water near the non-reactive carbon assists the hydration by hydrogen bonding with substrate. The best predicted activation Gibbs free energy in solution is 57.5 kJ/mol, compared to the experimental value of 63.0 kJ/mol.

To sum up, the explicit water molecules in the hydration of ketene not only take part in the proton transfer in the active region, but also interact among themselves in the non-reactive region to catalyze the hydration of ketene. Accordingly, it is necessary to consider the effect the cooperative role of the solvent molecules for the hydration of ketene, as in the hydration of other cumulenes containing heteroatom, such as NH=C=NH, O=C=O, O=C=S and S=C=S. The bulk solvent effect described by CPCM formulation modifies the calculated energy barriers in a significant way when the rate-determining TSs have dipole moments larger than those of the corresponding pre-complexes.

Acknowledgments This work is supported by a Strategic Grant (Project No. 7002334) awarded to NBW by City University of Hong Kong.

References

1. Matsunaga H, Kiyoshi Ikeda, Iwamoto KI, Suzuki Y, Sato M (2009) Tetrahedron Lett 50:2334
2. Nahmany M, Melman A (2001) Org Lett 3:3733
3. Cevasco G, Thea S (1994) J Org Chem 59:6274
4. Frey J, Rapport Z (1996) J Am Chem Soc 118:5169
5. Shelkov R, Nahmany M, Melman A (2002) J Org Chem 67:8975
6. Finnerty JJ, Wentrup C (2005) J Org Chem 70:9735
7. Orlova G, Blagojevic V, Bohme DK (2006) J Phys Chem A 110:8266
8. Markb I, Ronsmans B, Heshbain-Frisque A-M, Dumas S, Ghosez L, Ernst B, Greuter H (1985) J Am Chem Soc 107:2192
9. AI-Husaini AH, Moore HW (1985) J Org Chem 50:2595
10. Abbiati G, Contini A, Nava D, Rossi E (2009) Tetrahedron 65:4664
11. Lu J, Xue Y, Zhang H, Kim CK, Xie DQ, Yan GS (2008) J Phys Chem A 112:4501
12. Taggi AE, Hafez AM, Wack H, Young B, Ferraris D, Lectka T (2002) J Am Chem Soc 124:6626
13. Cannizzaro CE, Houk KN (2004) J Am Chem Soc 126:10992
14. Baigrie LM, Lenoir D, Seikaly HR, Tidwell TT (1985) J Org Chem 50:2105
15. Baigrie LM, Seikaly HR, Tidwell TT (1985) J Am Chem Soc 107:5391
16. Ma NL, Wong MW (2000) Eur J Org Chem 1411
17. Gong L, McAllister MA, Tidwell TT (1991) J Am Chem Soc 113:6021

18. Morales G, Martinez R (2009) J Phys Chem A 113:8683
19. Bouma WJ, Nobes RH, Radom L, Woodward CE (1982) J Org Chem 47:1869
20. Bothe E, Dessouki AM, Schulte-Frohlinde D (1980) J Phys Chem 84:3270
21. Frey J, Rappoport Z (1995) J Am Chem Soc 117:1161
22. Allen AD, Tidwell TT (1987) J Am Chem Soc 109:2774
23. Chiang Y, Fedorov AV, Kresge AJ, OnyidoI TidwellTT (2004) J Am Chem Soc 126:9382
24. Acton AW, Allen AD, Antunes LM, Fedorov AV, Najafian K, Tidwell TT, Wagner BD (2002) J A Chem Soc 124:13790
25. Chiang Y, Kresge AJ, Nikolaev VA, Popik VV (1997) J Am Chem Soc 119:11183
26. Chiang Y, Kresge AJ, Meng Q, Morita Y, Yamamoto Y (1999) J Am Chem Soc 121:8345
27. Chang JA, Kresge AJ, Nikolaev VA, Popik VV (2003) J Am Chem Soc 125:6478
28. Chiang Y, Guo HX, Kresge AJ, Tee OS (1996) J Am Chem Soc 118:3386
29. Raspoet G, Nguyen MT (1998) J Org Chem 63:9669
30. Rodriguez-Otero J, Hermida-Ramon JM, Cabaleiro-Lago EM (2007) Eur J Org Chem. 2344
31. Nguyen MT, Hegarty AF (1984) J Am Chem Soc 106:1552
32. Skancke PN (1992) J Phys Chem 96:8065
33. Nguyen MT, Raspoet G (1999) Can J Chem 77:817
34. Nguyen MT, Matus MH, Jackson VE, Ngan VT, Rustad JR, Dixon DA (2008) J Phys Chem A 112:10386
35. Nguyen MT, Raspoet G, Vanquickenborne LG, Van Duijen PT (1997) J Phys Chem A 101:7379
36. Merz KM (1990) J Am Chem Soc 112:7973
37. Liang JY, Lipscomb WN (1986) J Am Chem Soc 108:5051
38. Lewis M, Glaser R (2003) J Phys Chem A 107:6814
39. Deng C, Li QG, Ren Y, Chu WongNB, SY ZhuH (2008) J Comput Chem 29:466
40. Deng C, Wu XP, Sun XM, Ren Y, Sheng YH (2009) J Comput Chem 30:285
41. Lewis M, Glaser R (1998) J Am Chem Soc 120:8541
42. Lewis M, Glaser R (2002) Chem Eur J 8:1934
43. Tordini F, Bencini A, Bruschi M, Gioia LD, Zampella G, Fantucci P (2003) J Phy Chem A 107:1188
44. Nguyen MT, Raspoet G, Vanquickenbome LG (1999) J Chem Soc Perkin Trans 2:813
45. Barone V, Cossi M (1998) J Phys Chem A 102:1995
46. Rappe AK, Casewit CJ, Colwell KS, Goddard WAIII, Skiff WM (1992) J Am Chem Soc 114:10024
47. Frisch MJ, Trucks GW, Schlegel HB, Scuseria GE, Robb MA, Cheeseman JR, Montgomery JA Jr , Vreven T, Kudin KN, Burant JC, Millam JM, Iyengar SS, Tomasi J, Barone V, Mennucci B, Cossi M, Scalmani G, Rega N, Petersson GA, Nakatsuji H, Hada M, Ehara M, Toyota K, Fukuda R, Hasegawa J, Ishida M, Nakajima T, Honda Y, Kitao O, Nakai H, Klene M, Li X, Knox JE, Hratchian HP, Cross JB, Bakken V, Adamo C, Jaramillo J, Gromperts R, Stratmann RE, Yazyev O, Austin AJ, Cammi R, Pomelli C, Ochterski JW, Ayala PY, Morokuma K, Voth GA, Salvador P, Dannenberg JJ, Zakrewski G, Dapprich S, Daniels AD, Strain MC, Farkas O, Malick DK, Rabuck AD, Raghavachari K, Foresman JB, Ortiz JV, Cui Q, Baboul AG, Clifford S, Cioslowski J, Stefanov BB, Liu G, Liashenko A, Piskkorz P, Komaromi I, Martin RL, Fox DJ, Keith T, Al-Laham MA, Peng CY, Nanayakkara A, Challacombe M, Gill PMW, Johnson B, Cheng W, Wong MW, Gonzalez C, Pople JA (2003) Gaussian 03, Revision D.01. Gaussian Inc, Pittsburgh, PA
48. Mourik TV (2005) Chem Phys Lett 414:364
49. Reed AE, Curtiss LA, Weinhold F (1988) Chem Rev 88:899